THE AUTONOMOUS MINI HELICOPTER: A POWERFUL PLATFORM FOR MOBILE MAPPING

Henri Eisenbeiss

Institute of Geodesy and Photogrammetry, ETH Zurich, CH-8093, Zurich, Switzerland, +41 44 633 32 87
ehenri@geod.baug.ethz.ch

Commission Ⅰ, ICWG I/V

KEY WORDS: Acquisition, Automation, Integration, Mobile, Mapping, Processing, UAV

ABSTRACT:

In this paper, the developments related to an autonomous airborne mobile mapping system for photogrammetric processing will be presented. During the last years the author has been involved in several projects related to mobile mapping using an autonomously flying model helicopter, a so-called mini UAV (Unmanned Aerial Vehicle). The overall motivation of using mini UAVs for mobile mapping, the developed workflow for UAV-data processing, the current status of the work, and recent developments related to specific applications are described. In a first step our mini UAV-system and our approach are explained and the need for specific developments is highlighted. In the following two applications will be described: The Randa rockslide and the maize project, demonstrating our developments for the automation of the photogrammetric workflow using the mini UAV system. In the Randa project a unique flight planning tool for UAV-monitoring of mountainous areas was developed. The tool allows for the adaptation of the flight in a way, that image data with 2-3 cm resolution of the cliff could be acquired. Moreover, due to this high image resolution, a DSM with a higher point density compared to standard airborne and helicopter-based LIDAR-systems, could be generated. In the second project the focus was on the automation of the image orientation process. Hence, two test areas (A and B) were defined. While in A two commercial photogrammetric workstation were evaluated, in B the data set was processed using GPS/INS data as initial values for the image orientation. Therefore, the manual input for the aerial triangulation was reduced to a minimum user interaction. Finally, with the oriented image data two DSMs for the analysis of the outcrossing in maize were generated. Because of these developments, the tools for the planning and the data acquisition as well as the workflow for the processing of UAV-images were automated. However, the complete workflow still requires manual interaction, which will be discussed here in detail including a proposal for future developments.

1. INTRODUCTION

Throughout the last years, UAVs (Unmanned Aerial Vehicles) have become more and more suitable platforms for data acquisition in photogrammetry and mobile mapping. “UAVs are to be understood as uninhabited and reusable motorized aerial vehicles.” (van Blyenburg, 1999). These vehicles are remotely controlled, semi-autonomous, autonomous, or have a combination of these capabilities. The term UAV is used commonly in the computer science, robotics and artificial intelligence communities. Supplementary, in the literature also synonyms like Remotely Piloted Vehicle (RPV), Remotely Operated Aircraft (ROA) and Unmanned Vehicle Systems (UVS) can be found. The definition of UAVs encompasses fixed and rotary wings UAVs, lighter-than-air UAVs, lethal aerial vehicles, aerial decoys, aerial targets, alternatively piloted aircrafts and uninhabited combat aerial vehicles. Sometimes, cruise missiles are also referred to as UAVs (van Blyenburg, 1999).

However, a model helicopter was selected for our investigations. Model helicopters are clearly defined by the Unmanned Vehicle Systems (UVS) International Association as mini, close short and medium range UAVs depending on their size, endurance, range and flying altitude (UVS, 2008).

In contrast to standard airplanes, model helicopters are able to operate closer to the object. In addition, these systems are highly flexible in navigation compared to fixed wing UAVs (Bendea et al., 2007) and, in contrast to Microdrones (Nebiker et al., 2007), more stable against environmental conditions like wind. The developments of model helicopters and comparable autonomous vehicles are primarily driven by the artificial intelligence community (AAAI, 2008) and have been used mainly in the past for military applications with increasing use in the civilian sector.

In the past, model helicopters were already used in photogrammetric applications (Eisenbeiss, 2004). However at that time, the model helicopters were controlled manually via radio link. Nowadays, these new technologies allow low cost navigation systems to be integrated in model helicopters, enabling them to fly autonomously. This kind of autonomous flying model helicopter is called mini UAV system (Blyenburg, 1999; Eisenbeiss 2004). These mini UAVs are highly manoeuvrable due to the possibility of hovering, change of flight direction around the center of rotation as well as the capability for turning the mounted camera in horizontal and vertical direction. However, due to the difficulty of keeping the ideal position and attitude, the vibration of the helicopter and the manual planning of image acquisition points, model helicopters have not been used successfully in the past for measurements, precise modeling and mapping of objects (Eisenbeiss, 2004). Latest developments integrate GPS/INS (Global Positioning System / Inertial Navigation System) together with a stabilization platform for the camera. Because of the small size and the low payload, the selection of the installed hardware is mostly limited to low cost navigation systems with low precision. Nevertheless, the

combination of GPS/INS sensors with image data for navigation allows more precise and reliable results. Furthermore, the integration of GPS/INS and image data in a real time triangulation method will drastically reduce time and cost required for post processing.

Mini UAVs have been used recently for civilian applications like 3D city modeling (Wang et al., 2004), modeling of a medieval castle in Sarnen (Pueschel et al., 2008), Horcher and Visser (2004) proposed applications in forestry like BMP Inspections, road maintenance of forest roads and trespas**.** Further on, UAVs were used in applications related to agriculture (Herwitz et al., 2004; Rovira-Más et al., 2005; Eisenbeiss, 2007; Reidelstuerz et al., 2007; Rovira-Más et al., 2008) and for the documentation of an archaeological site (Lambers et al., 2007). In these projects the focus was on a fast data processing, which reduces the accuracy of the results or in contradiction the results had high accuracy, while the processing cost still a lot of manual effort.

Hence, our goal is the automation of the complete workflow in a way that the manual input can be reduced to an acceptable minimum. A further objective of our work is the high reliability, precision and resolution of the photogrammetric products like elevation models, orthophoto and textured 3D models. Therefore, the aim is to develop procedures for the UAV data acquisition and processing that can lead to a highly automated workflow and accurate complete results (see Figure 1).

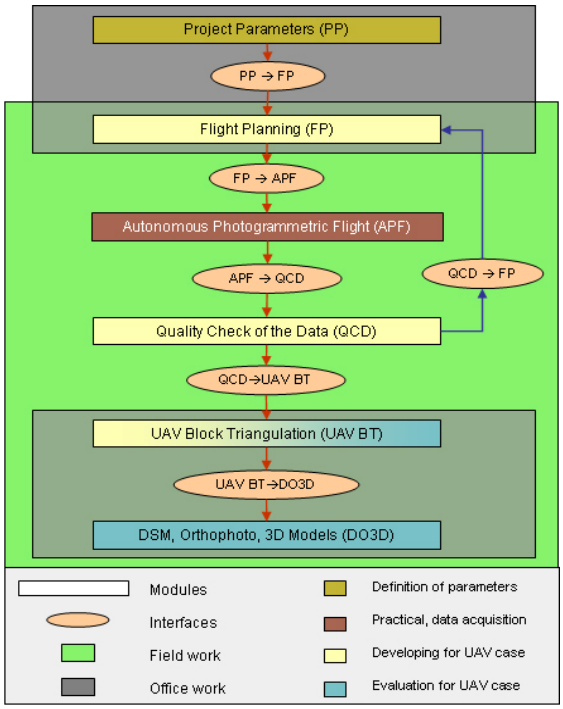

Figure 1: Modular Workflow for processing of UAV data showing the main functionalities.

All processing steps of the workflow are categorized in modules, which communicate with each other via interfaces. The interfaces are established in a way that for the individual module the attributes can change, depending on the project parameters. Additionally, the interfaces have the functionality for data transformation and formatting. Therefore, with our proposed workflow several UAV applications can be handled. The main modules are defined as follows: Project parameters (PP), Flight planning (FP), Autonomous photogrammetric flight (APF), Quality check of the data (QCD), UAV Block Triangulation (UAV BT), DSM, orthophoto, 3D Model (DO3D). The individual procedures of a module can be a process or a part of a process from commercial or in-house developed software.
Figure Figure 1 show which module are or will be developed by IGP and which focus more on the evaluation of existing commercial or in-house developed software packages. Additionally, figure 1 explains which part of the work will be possible during or after the field work or both.

In the following, two developments related to real applications of such a mini UAV-system, which lead to the automation of the workflow, will be presented. Before describing the developments in detail, our mini UAV-system and its ground control station will be described. After all, the outcome of the developments and the direct benefits using an UVS system in the two specific applications are discussed. Finally, we will propose a new UAV-platform, which can lift a bigger payload.

2. AUTONOMOUS MINI HELICOPTER

The mini UAV-system Copter 1b (see Figure 4 and Table 1) was developed by the French company Survey-Copter. It is equipped with an on-board navigation system (wePilot 1000) from weControl. The wePilot includes a GPS (Global Positioning System), an INS (Inertial Navigation System), which allows the mini UAV to perform attitude stabilization, position control and to navigate autonomously. The private company weControl GmbH is a spin-off of ETH Zurich that specialized in the development of miniature flight control systems for UAV-systems.

Mini UAV-system Copter 1b	
Length	2m
Rotor diameter	1.8m
Maximum takeoff weight	15kg
Payload capacity	5kg
Flight endurance	Max. 45min
Altitude	1500m
Range	5km

Table 1: Specifications of the mini UAV Copter 1b (SurveyCopter, 2008).

The navigation system features the following main characteristics: an altitude stabilization and velocity control, position and RC transmitter sticks interpreted as velocity commands, integrated GPS/INS system, altimeter, magnetometer, payload intensive flight controller, built-in data logger and telemetry capability, programmable hardware for rapid customization and an embedded computer system. Furthermore, the system consists of a ground control station (a laptop with monitoring software (weGCS)), a convertible gimbal for still video cameras like Canon EOS D10, D20 and the Nikon D2Xs, communication links, power supply, video link (incl. video camera) for visual control for monitoring image overlap, and transport equipment.

The ground control station also includes a flight simulator, which allows the simulation of the real flight to verify the predefined flight path (see Figure 2).

3. RANDA

3.1 Project Aims

The focus of the geological project Randa is to characterize the large-scale rockslide in Randa (Wallis, Swiss Alps; see Figure 3). This rockslide will be used as an example of the ultimate evolutionary stages corresponding to the complete development of the basal shear surface(s) and internal rock mass deformation. In order to understand this failure stage in a better way, the interrelationships between pre-existing tectonic fractures, subsequent tensile fracturing and shearing of intact rock bridges will be investigated. Furthermore, for the understanding of the rock mass structure and kinematics during this evolutionary stage, the basal shear planes must be identified, the internal rock mass deformation has to be further studied, and the 3D time-dependent displacement field has to be measured more in detail using the UAV-image data and the generated DSM (Randa, 2008).

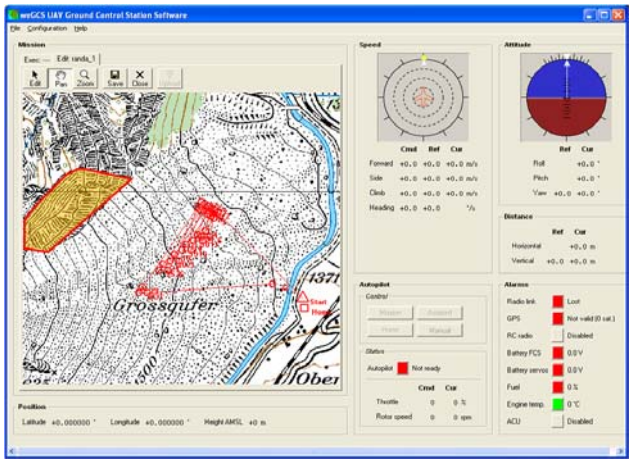

Figure 2: Screenshot of the ground control station software showing the flight lines of the Randa data acquisition. In off-line mode the software can be used for the simulation of the flight. The orange shading shows the lower part of the Randa rock cliff.

Figure 3: The Randa rockslide failure (Wallis, Switzerland). The lower part is situated 1400 a.s.l. The height difference from the bottom to the top is more than 800m.

Therefore, a high-resolution digital surface model (DSM) with a spatial resolution of 10–20cm had to be generated and oriented images with a footprint of 2-5cm in object space had to be acquired. Because of the non-nadir case and a difficult terrain, the standard aerial flight planning procedures could not be applied.

Furthermore, the sight was acquired by a manned helicopter in November 2007, using the Helimap system, combining laser scanning and oblique images (Vallet, 2007). The system is based on a Riegl LMS-Q240i-60 laser scanner for point cloud generation and a Hasselblad H1 camera with a Dos Imacon Xpress 22Mpix back, which is normally used for texture mapping.

Using the two comparable systems, the autonomous flying model helicopter and the manned helicopter, at one site, allowed the analysis of the performance of the systems. Moreover, it is possible to compare and integrate the two data sets.

3.2 Flight planning

Before doing the flight, the main parameters of the autonomous flight were defined. For the Randa rockslide we decided to use the Nikon D2Xs, which has a CMOS-sensor with 4288x2848 pixels using a 50mm lens (Nikon, AF NIKKOR 50mm 1:1.8D) and a pixel size of 5.5µm. For the recognition of features with a length of 10-20cm, an image scale of 1:4500 was selected which results in a pixel footprint of approximately 3cm. The distance to the cliff was defined to 230m, which is equal to the normally used flying height above ground. Finally, the side and end lap were set to 75%. Using this high overlapping along and across strip it was possible to avoid occlusions and gaps in the image data (see Figure 6). The flight velocity was defined to 3m/s, while the shutter speed was 1/1000s. Therefore, the influence of the image motion was negligible.

After defining these parameters, the most recent elevation model with the highest available point density was used. Therefore, the LiDAR data provided by swisstopo was selected. Using this data set and the available orthophoto (swissimage, swisstopo®) allowed the definition of the area of interest. Hence, the area was separated in three sections. The sections were selected using the inclination and aspect values of the slope.

Figure 4: Our model helicopter during a test flight with the inclined camera looking perpendicular to the flight direction.

For each particular section a plane was defined in a way that the average 3D distance of the surface to the plane was reduced to a minimum. While looking perpendicular to the surface, we assumed to reduce the occlusion in the images. After the definition of the plane equation, the normal of the plane was

calculated and with the given flying distance to the surface a parallel plane was defined (see Figure 5). In the new plane the area of interest was projected and the inclined flight lines for the helicopter flight were generated. Finally, using this information the image acquisition points were determined and transferred to the navigation unit (wePilot1000) of the mini UAV-system. Due to the inclination of the plane the camera was mounted with a pitch angle of 15-30° (respectively for the individual sections) on the helicopter (see Figure 4).

Such precise planning was necessary due to the large distance between operator and mini UAV, which limited the visibility of the mini UAV. Furthermore, before flying along the predefined flight path, the mini UAV was tested at an altitude of 2400m a.s.l. in order to ensure that the engine of the helicopter would not fail due to low air pressure. This test was important, since the helicopter manufacturer set the maximum flying altitude to 1500m a.s.l. In the following, the results from the first flight in Randa and an elevation model extracted from the acquired data will be described.

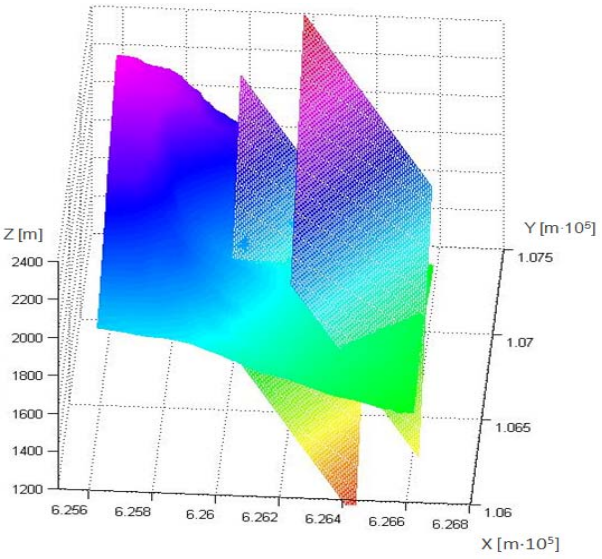

Figure 5: Zoom-in to one section of the cliff showing the LiDAR-DSM with the approximated and parallel plane from the flight planning.

3.3 Field Work

Since the Randa rockslide covers a height from 1400m -2300m a.s.l. the mini UAV-system was tested at the Flueelapass (~2400m a.s.l., Graubuenden, Switzerland). For the flight at Flueelapass weight dummies instead of the mounted camera were used on the helicopter. To enable the evaluation of the performance at such a height above mean sea level, the helicopter was started and switched to the assisted flying mode. In this mode the current parameters of the engine were checked visually and saved on board of the helicopter. This specific test showed that the engine of our mini UAV-system already achieved the limit for the maximal turning moment of the engine. Therefore, to have a buffer, we decided to do the first flight only at the lower part of the rockslide (1400-1800m a.s.l., see Figure 3), while the upper part was also covered by the Helimap flight.

Since the illumination conditions were acceptable only in the morning, we decided to do the flight at Randa in the morning hours. In the afternoon strong shadows made the data processing more complicated, while a preprocessing of shadow areas had to be accomplished. Furthermore, the GPS-satellite availability was simulated in the preparation process. Thus, the existing elevation model of the surrounding (DHM25, swisstopo®) was integrated in a GPS sky plot software, which allowed the calculation of the accessible number of GPS and the postulated GDOP (Geometric Dilution Of Precision) value. Using this information, it was possible to have an approximate a-posteriori value for the accuracy of the GPS-position of the helicopter, which was crucial in such an environment.

Given that at the bottom the site a large debris zone is situated (see Figure 3), the accessibility of the site is quite complicated. Therefore, the start and landing point was defined close to a road at the bottom of the debris zone (see Figure 2). The field work itself was done in few minutes, while the longest part of the flight was the way to go from the starting point to the first image acquisition point and the way back. At the end of the first flight, the helicopter did a fast in-explainable turn along its own main axis. Hence, we decided to stop the test and to evaluate the flight data, having already the first high resolution images from the rockslide.

Figure 6: Left: Derived surface model from image matching, Middle: Zoom-in of an UAV-image, Right: Point cloud of Helicopter-based LiDAR projected on the derived surface model.

3.4 Results

Using the acquired UAV-images, a DSM of the lower part of the Randa rockslide with 15cm resolution was generated (see Figure 6). The complete site was documented with the Helimap system. For the Helimap system, the pixel size was 6cm to 8cm. In comparison to the flight defined for the mini UAV-system, the Helimap flight was controlled by a pilot, who followed the flight lines with an accuracy of 30m. Therefore, for the whole area the scale varies depending on the complexity of the terrain. Furthermore, the Helimap system acquired the cliff with an oblique field of view, which evokes the gaps through occlusion in the data set. For the laser scan, the final point density was approximately 3pt/m^2 (see Figure 6).

The visual comparison of the extracted UAV-DSM and the LiDAR-DSM shows clearly that the fine structure of the cliff could be modeled out of the UAV-DSM, while the LiDAR-DSM shows big holes and less resolution (see Figure 6).
The analysis of the unexpected turning of the UAV-system during the flight showed that the effect was caused by the fact that the neighboring points of the flight plan were defined to close to each other. Furthermore, the effect evoked while the neighboring flight lines had a distance in horizontal and vertical direction, which caused a miss-interpretation in the flight control software. Hence, during the flight, one predefined data acquisition point was skipped and the turning occurred during the flight at Randa. Therefore, the flight control software was improved to handle autonomous flights flown with this type of configuration.

4. MAIZE FIELD

4.1 Project Aims

The goal of this study was to analyze the influence of terrain characteristics on pollen dispersal in maize. For that application, the task was to generate 3D elevation models as well as to use the oriented images for a stereoscopic inspection of maize fields, and to combine them with high resolution cross-pollination data. The elevation model and the stereoscopic measures were used to determine the heights of pollen donor and receptor plants with respect to their absolute orthometric height. For these investigations, two test areas (2005: A and 2006: B) were defined.

Parameter	Value
Image scale	1:4000
Side / end lap	75% / 75 %
Flying height above ground	~ 80 m
Camera	Canon EOS 20D
Focal length (calibrated)	20.665, RMSE 1.5e-003 mm
Pixel (Image format)	8.25 megapixels (3520x2344)
Flying velocity	3 m/s

Table 2: Flight parameters for the image observation of the maize field in 2005 and 2006

4.2 Field work

After anthesis, digital pictures were captured with a still-video camera (Canon D20) mounted on our mini UAV-system (Eisenbeiss, 2007).

In the first step, a flight planning was performed for the autonomous flight. The image resolution was defined to have 3 cm per pixel in object space. Furthermore, the maximum flying height was set to 100m above ground, due to the nearness to Zurich airport. With the selected camera the remaining parameters were calculated (see Table 2) **.**

After definition of the flight parameters, the area of interest was roughly identified in the Swiss National Map 1: 25 000 provided by swisstopo. With the defined flight parameters, a trajectory was calculated by starting at one corner of the field and 3D-coordinates of the flight trajectory were established. The autonomous flight was done using our UAV system. Following the flight trajectory in the stop mode for experiment A, the camera captured the images automatically on the predefined positions in the cruising flight mode for experiment B. In the stop mode the helicopter flew autonomously to each image acquisition point and the operator triggered the image via radio link, while during the cruising mode the image acquisition was completely autonomous.

4.3 Data Processing

Due to the autonomous flight with stop points we could capture all images for experiment A in 20 minutes. By using the cruising flight modus we reduced the flight time for experiment B to 5 minutes.

For the image triangulation for experiment A 2-3 tie points were measured manually, while for the experiment B the orientation values calculated using the Kalman filter implemented in the navigation unit on board the mini UAV were used. For 5-10 percent of the images the 2-3 manually measured points were not enough, since during the image acquisition the light breeze moved the leaves of the plants slightly. Therefore, the measurement of more manual points was essential (Eisenbeiss, 2007). The manually measured points (experiment A) and the approximate positions of the camera (experiment B) served as initial values for automated tie point extraction. For the generation of the tie points, the standard procedure implemented in LPS (Leica Photogrammetry Suite) was used. Therefore, the initial approximations of each image location within the projects had to be defined. Hence, for area B the function for exterior orientation parameter input and for area A the function for manual tie point measurement were selected. After the generation of tie points, the control points were manually measured in the images.

Since the maize fields had a highly repetitive structure in the image, it was necessary to detect blunders before doing image orientation. In LPS, a blunder can be detected only by manual checking until the project has proceeded to the point where a bundle adjustment is possible. Therefore the blunder detection with ORIMA (Leica Geosystems) integrated in LPS and ISDM (Image Station Digital Mensuration, Intergraph) was attempted. These software packages allow a relative orientation for each stereo pair, multi-image blocks and the detection of blunders. Finally, with both software packages the blunders were detected and the orientation of the UAV-images was performed with an

sigma 0 a posteriori of approx. 0.5 pixel and the RMS error for the control points was below 1dm for both test areas.

4.4 Results

After image orientation, a DSM with a resolution of 10 cm was produced automatically with the in-house developed software package SAT-PP (Satellite imagery Precise Processing). The software was initially developed for the processing of satellite images and later adapted such that it was capable to handle still-video camera and aerial images. Due to the combination of the multi image approach and the combination of different matching methods (area, feature and edge matching) (Zhang, 2005) allowed the generation of a precise, reliable and consistent 3D model of the maize field. Finally, an orthophoto with a footprint of 3 cm was produced using the generated DSM and integrated into a GIS for further analysis (see Figure 7).

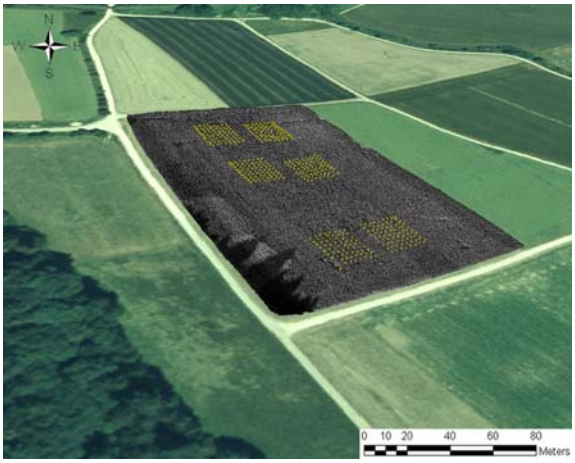

Figure 7: Screenshot of the 3D-model of experiment B (2006) using the Swissimage orthoimage (swisstopo®) draped over the DHM25 (swisstopo®) combined with the orthoimage of the maize field and the position of the cross-pollination data.

5. CONCLUSIONS AND FUTURE WORK

In this study, a workflow for the processing of UAV data was presented. The processing steps of the workflow are based on modules, which allow the independent adaptation of the individual steps.

The autonomous flight allowed us to predefine the flight trajectory for an optimal photogrammetric processing. The flight trajectories for both projects were calculated automatically by in-house developed software using existing topographic maps, orthophotos and elevation models. For the Randa project, the flight planning was modified to the non-nadir case. Two autonomous flying modes were applied in the maize field project: stop modus and cruising modus. By using the cruising mode the flight time could be reduced by 75 percent for the observation of one field. The performance of the system during the cruising mode is comparable with fixed-wing UAV systems (Horcher and Visser, 2004), while the stabilizer system of the helicopter allowed a continuous and stabilized flight. In addition, the helicopter system is more flexible than comparable fixed wing systems due to the system characteristics. Therefore, the used autonomous flying helicopter system can be introduced in several applications like crop maps for biomass measurement, as input for tractor-automated guidance (Kise et al., 2005), in forestry, for monitoring and detection and prediction of erosion using the extracted image data, orthophotos and elevation model. Furthermore, the mini UAV-system can be used for 3D city modeling in combination with an autonomous car (Lamon et al., 2006).

In comparison to the mobile stereovision system, proposed by Rovira-Mas et al. (2005) and Rovira-Mas et al. (2008), our method allows an autonomous documentation with the UAV system by producing accurate and reliable elevation models and orthoimages of the site. The produced data can be directly integrated into several GIS systems using absolute coordinates. Therefore, the data can be easily combined with any other reference data. Furthermore, by using medium format still-video cameras, the image and the derived DSM resolution allows analysis at a larger scale as with stereovision systems using the same flight height. Therefore, large sites can be documented completely in a shorter time period with our method.

Orientation values were calculated by using the Kalman filter implemented in the navigation unit on board the mini UAV as initial exterior orientation parameters for the photogrammetric processing for experiment B; we could reduce the manual effort during the photogrammetric processing. However, the complete workflow still requires manual measurements for the control points and statistical analysis of the results. This lack of automation has to be the emphasis for future work by development of online-triangulation methods and the automated measurements of control points using coded targets.

In future work, we will also focus on the combination of LiDAR and image data. Since our model helicopter has a maximum payload of 5kg, a more powerful UAV-system (Aeroscout Scout B2-120; Aeroscout) will be used, which also features the flight control system of weControl. The combination of LiDAR and image data allows us to use the strength of both systems: the laser scanner is good in areas with less texture, while image data is advantageous for edge measurement and texture mapping.

ACKNOWLEDGEMENTS

The author thanks Kirsten Wolff and Martin Sauerbier for their contribution to the paper and Manuel Kaufmann for his input to the Randa project.

REFERENCES

AAAI. 2008. American Association for Artificial Intelligence. http://www.aaai.org (accessed May 8th 2008).

Bendea, H. F., Chiabrando, F., Tonolo, F. G., Marenchino, D., 2007. Mapping of archaeological areas using a low-cost UAV the Augusta Bagiennorum Test site. XXI International CIPA Symposium, Athens, Greece.

Eisenbeiss, H., 2004. A mini unmanned aerial vehicle (UAV): system overview and image acquisition. International Archives of Photogrammetry. *Remote Sensing and Spatial Information Sciences*. 36(5/W1). (on CD-ROM).

Eisenbeiss, H., 2007. Applications of photogrammetric processing using an autonomous model helicopter. Revue Francaise de Photogrammetrie et de Teledetection. Symposium ISPRS Commission Technique I "Des capteurs a l'Imagerie", n°185 (2007-1), Saint-Mande Cedex, France.

Herwitz, S.R., Johnson, L.F., Dunagan, S.E., Higgins, R.G., Sullivan, D.V., Zheng, J., Lobitz, B.M., Leung, J.G., Gallmeyer, B., Aoyagi, M., Slye, R., E., Brass, J., 2004. Demonstration of UAV-based imaging for agricultural surveillance and decision support. *Comput. Electron.* Agr. 44:49-61.

Horcher, A., Visser, R.J.M., 2004. Unmanned aerial vehicles: Applications for natural resource management and monitoring. COFE (Council on Forest Engineering) *Annual Meeting* 2004, Proceedings; http://www.cnr.vt.edu/ifo/VT%20Andy%20COFE%202004%20Drone%20Paper1.pdf (accessed 08. May 2008).

Kise, M., Rovira-Más, F., Zhang, Q., 2005. A stereovision-based crop row detection method for tractor-automated guidance. *Biosystems Eng.* 90:357-367.

Lambers, K., Eisenbeiss, H., Sauerbier, M., Kupferschmidt, D., Gaisecker, T., Sotoodeh, S., Hanusch, T., 2007. Combining photogrammetry and laser scanning for the recording and modelling of the late intermediate period site of Pinchango Alto, Palpa, Peru. J. Archaeol. Sci. 34:1702-1710.

Lamon, P., Stachniss, C., Triebel, R., Pfaff, P., Plagemann, C., Grisetti, G., Kolski, S., Burgard, W., Siegwart, R. 2006. "Mapping with an Autonomous Car", Proc. of The Workshop on Safe Navigation in Open and Dynamic Environments (IROS).

Nebiker, S., Christen, M., Eugster, H., Flückiger, K. and Stierli, C., 2007. Integration von mobilen Geosensoren in kollaborative virtuelle Globen, Dreiländertagung der SGPBF, DGPF und OVG: Von der Medizintechnik bis zur Planetenforschung - Photogrammetrie und Fernerkundung für das 21. Jahrhundert. DGPF Tagungsband Nr. 16, FHNW, Muttenz, pp. 189-198.

Pueschel, H., Sauerbier, M., Eisenbeiss, H., 2008. A 3D model of Castle Landenberg (CH) from combined photogrammetric processing of terrestrial and UAV-based images. XXI ISPRS Congress , Beijing, China, 03.-11. July 2008, (In Press).

Randa rockslide, 2008. http://www.rockslide.ethz.ch/ (accessed May 8th 2008).

Reidelstuerz, P., Link, J., Graeff, S., Claupein, W., 2007. UAV (unmanned aerial vehicles) für Präzisionslandwirtschaft. 13. Workshop Computer-Bildanalyse in der Landwirtschaft & 4. Workshop Precision Farming 61:75-84.

Rovira-Más, F., Zhang, Q., Reid, J.F., 2005. Creation of three-dimensional crop maps based on aerial stereoimages. Biosystems Eng. 90:251-259.

Rovira-Más, F., Zhang, Q., Reid, J.F., 2008. Stereo vision three-dimensional terrain maps for precision agriculture. *Comput. Electron. Agr.* 60:133-143.

SurveyCopter, 2008. http://perso.wanadoo.fr/survey-copter/eindex.htm (accessed May 8th, 2008).

UVS International, 2008. Unmanned Vehicle Systems International http://www.uvs-international.org (accessed 08. May 2008).

Vallet, J., 2007. GPS-IMU and LiDAR integration to aerial photogrammetry: Development and practical experiences with Helimap System®, Voträge Dreiländertagung 27. Wissenschaftlich-Technische Jahrestagung der DGPF. 19-21 June 2007, Muttenz.

van Blyenburg, P., 1999. UAVs: an Overview. Air & Space Europe. Vol. I No 5/6. pp. 43-47.

Wang, Y., Yang, X., Stojic, A., Skelton, B., 2004. Toward higher automation and flexibility In commercial digital photogrammetric systems. IAPRS, Vol. XXXV, p. 838-840, Istanbul.

Zhang, L., 2005. Automatic Digital Surface Model (DSM) Generation from Linear Array Images. Ph. D. Dissertation, Institute of Geodesy and Photogrammetry, ETH Zurich, Switzerland, Report No. 88.